



BDM Dark Matter (solving CDM problems)

Axel de la Macorra

Instituto de Física, UNAM

Instituto Avanzado de Cosmología

PASCOS 2012, Merida

Collaborators and References

- Jorge Cevantes (ININ, Mexico)

Students

- Jorge Mastache (UNAM, Mexico)
- Jesus Cereceres (UNAM, Mexico)

References:

- **BDM Dark Matter: CDM with a core profile and a free streaming scale**
A. de la Macorra, [Astropart.Phys. 33:195-200,2010.](#)
- **Galactic Phase Transition at $E_c = 0.11$ eV from Rotation Curves of Cored LSB and nonperturbative Dark Matter Mass.**
A. de la Macorra, J. Mastache, J. Cervantes.
PRD Rapid Communications: [Phys.Rev. D84 \(2011\) 121301](#)
- **Core-Cusp revisited and Dark Matter Phase Transition Constrained at 0.11 eV with LSB Rotation Curve.**
J. Mastache, A. de la Macorra, J. Cervantes [arXiv:1107.5560](#)
- **High-Resolution Rotation Curves and Galaxy Mass Models from THINGS.** De Blok et al [Astrophys. J. 136, 2648, 2008](#)

Evidence for Dark Matter

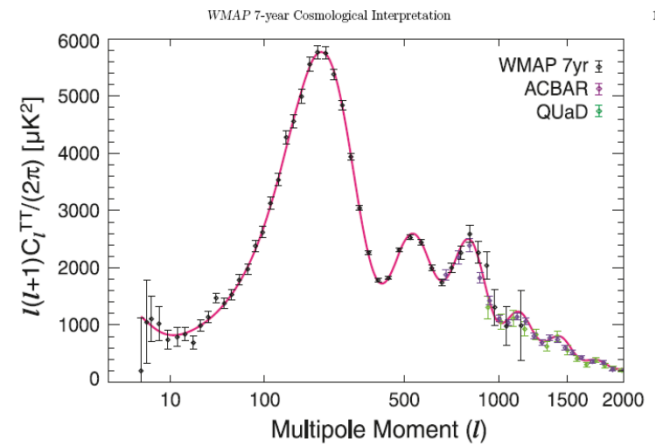
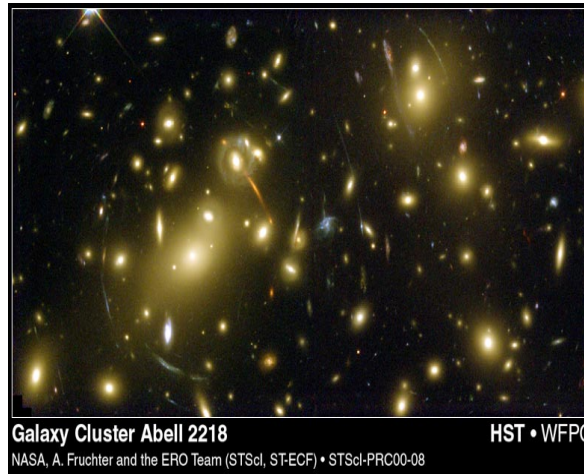
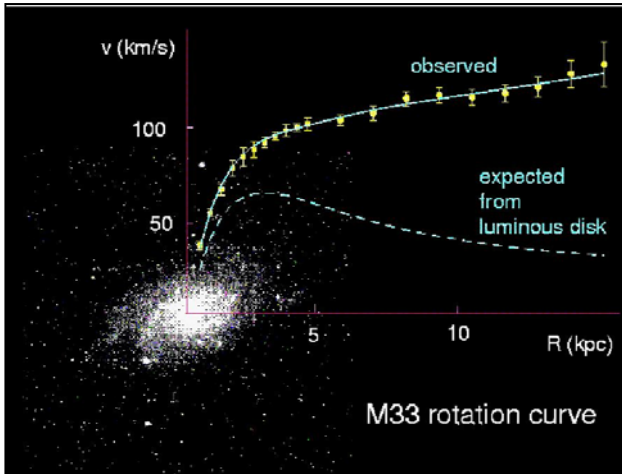
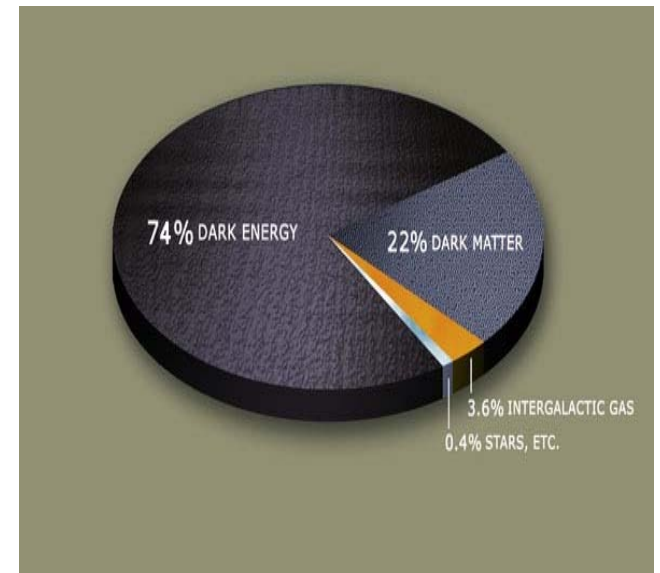
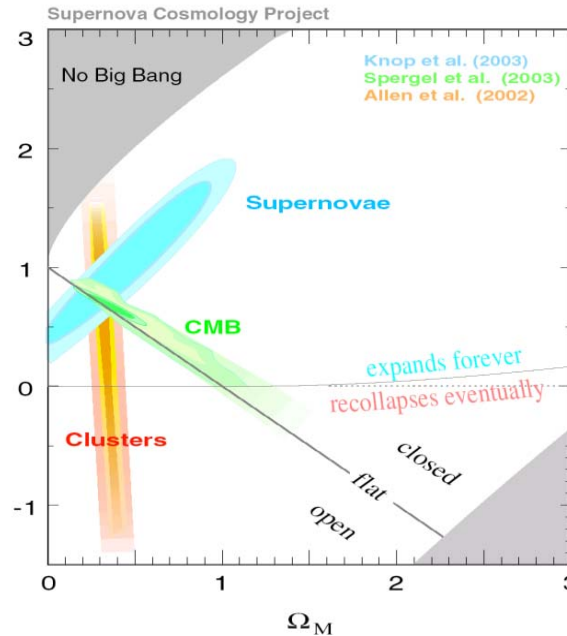
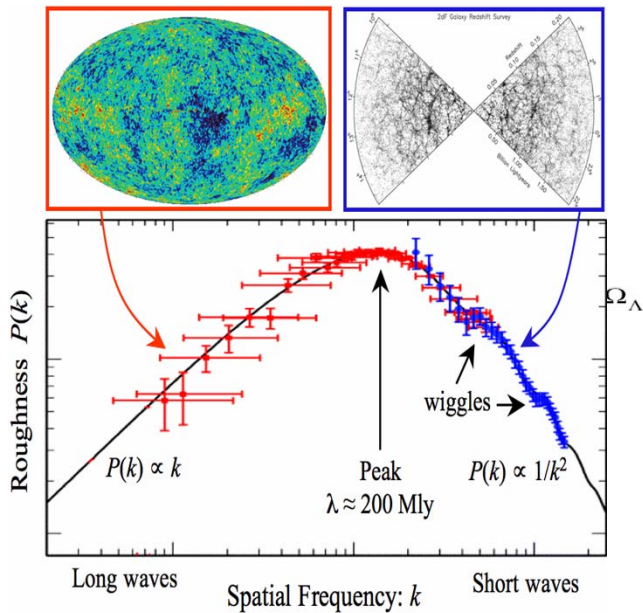


FIG. 7.— The WMAP 7-year temperature power spectrum (Larson et al. 2010), along with the temperature power spectra from t ACBAR (Reichardt et al. 2009) and QUaD (Brown et al. 2009) experiments. We show the ACBAR and QUaD data only at $l \geq 690$, where the errors in the WMAP power spectrum are dominated by noise. We do not use the power spectrum at $l > 2000$ because of a potential contribution from the SZ effect and point sources. The solid line shows the best-fitting 6-parameter flat Λ CDM model to the WMAP data alone (see the 3rd column of Table 1 for the maximum likelihood parameters).

Rotation curves in galaxies and cluster of galaxies , weak and strong lensing, CMB, Structure Formation, BAO ...



Dark Matter

Type of Dark Matter

- **CDM** Massive particle with vanishing dispersion speed $v = 0$ **ok**
(standard DM and with Λ CDM is the “concordance cosmological model”)
e.g. WIMPS (susy particles, axions etc) typical $m > \text{GeV}$
- **HDM** Relativistic particles with dispersion speed $v=c$ **NOT ok**
structure on small scales cannot grow
e.g. neutrinos $m=O(\text{eV})$
- **Warm WDM** Particles with mass $m=O(\text{keV})$ **ok**
- **BDM (Bound Dark Matter)**
particles which acquire a non perturbative (large) mass M (with $M \gg m_0$)
at a phase transition scale E_c
- e.g. $m = m_0$ for $E > E_c$
 $m = m_0 + M$ for $E < E_c$

as for example protons and neutrons

CDM or BDM

AT THE BEGINNING OF THE UNIVERSE

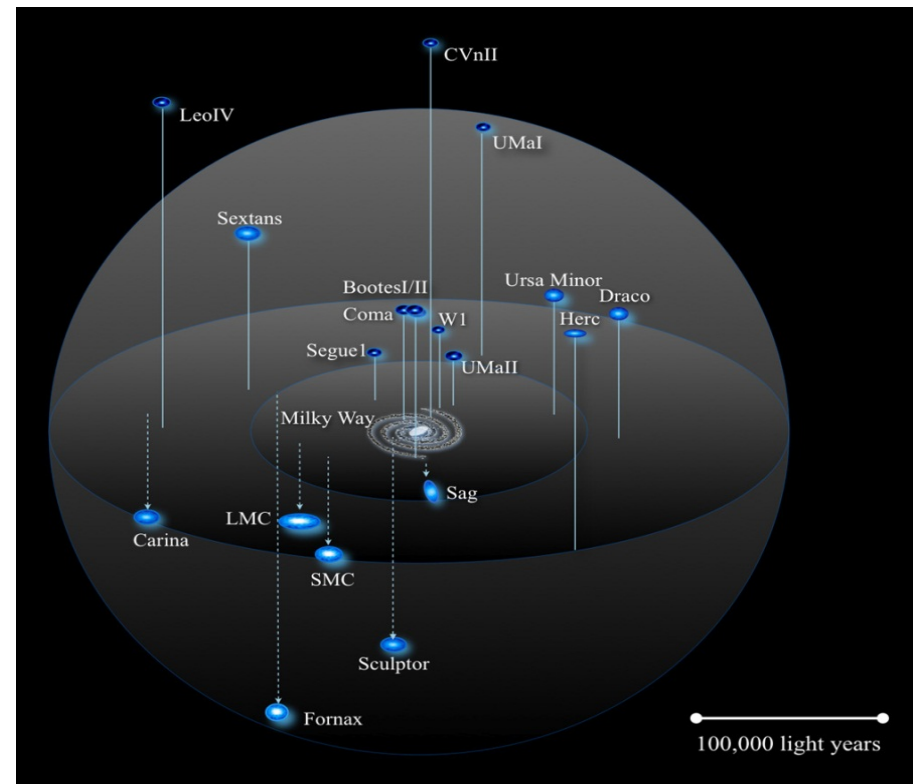
Problems of CDM:

- 1) Too much substructure
- 2) Cuspy vs Core DM profile
(many DM dominated galaxies show a core profile)

Can they have a common answer ?

Substructure:

CDM predicts a large number of small galaxies which are not seen (satellite galaxies)

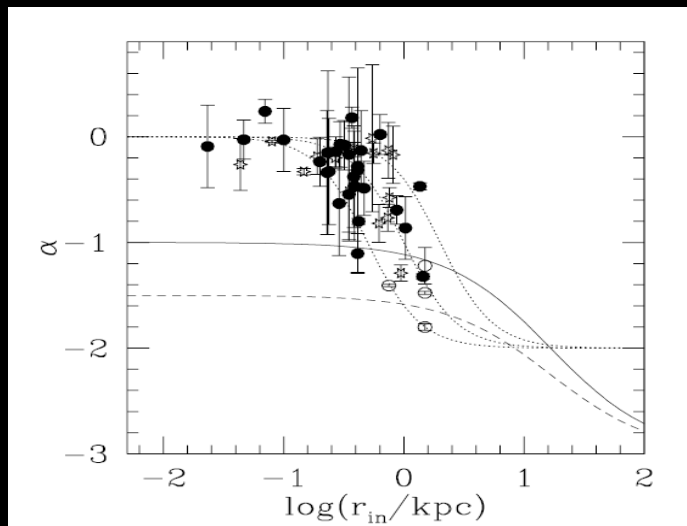
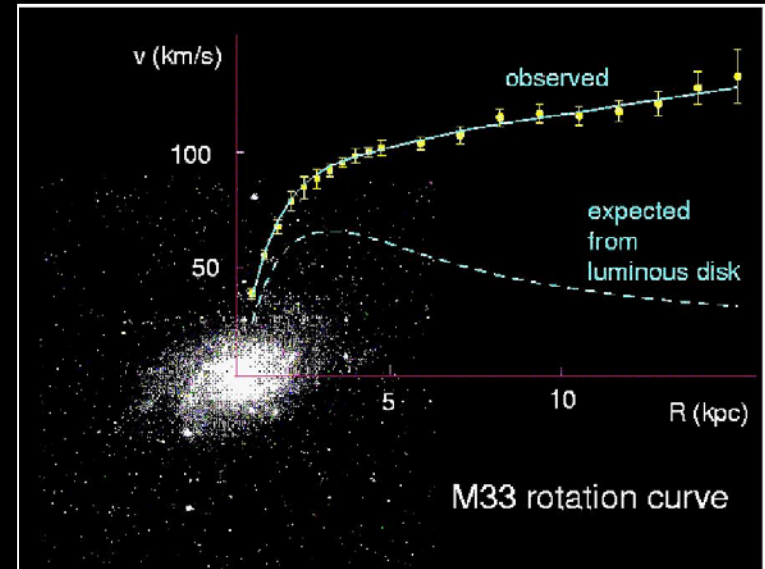


Galactic Rotation Curves => missing matter (Dark Matter)

$$v_{el} = \sqrt{\frac{GM(r)}{r}}$$

CDM has NFW cuspy profile
(not preferred by data)

$$\rho_{NFW} = \frac{\rho_0}{\frac{r}{r_s} \left(1 + \frac{r}{r_s}\right)^2}$$



$$\alpha \equiv \frac{d \text{Log}[\rho]}{d \text{Log}[r]}$$

de Blok et al 01

BDM: Bound Dark Matter

Phase transition at E_c

Phase transition at

$$\rho_c = E_c^4$$

BDM particles behave as

=

Radiation as HDM, $w=1/3$
above the scale energy E_c
with $m = 0$

$$\rho \propto a^{-4} \geq \rho_c$$

$$v \rightarrow c$$

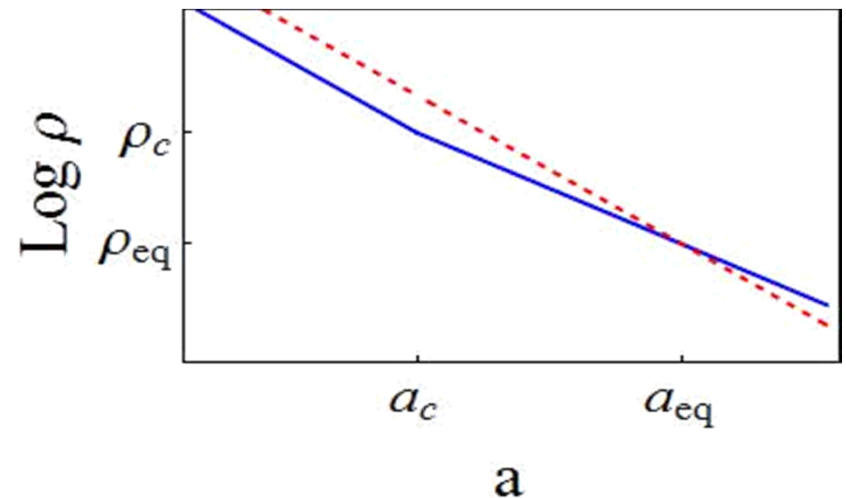
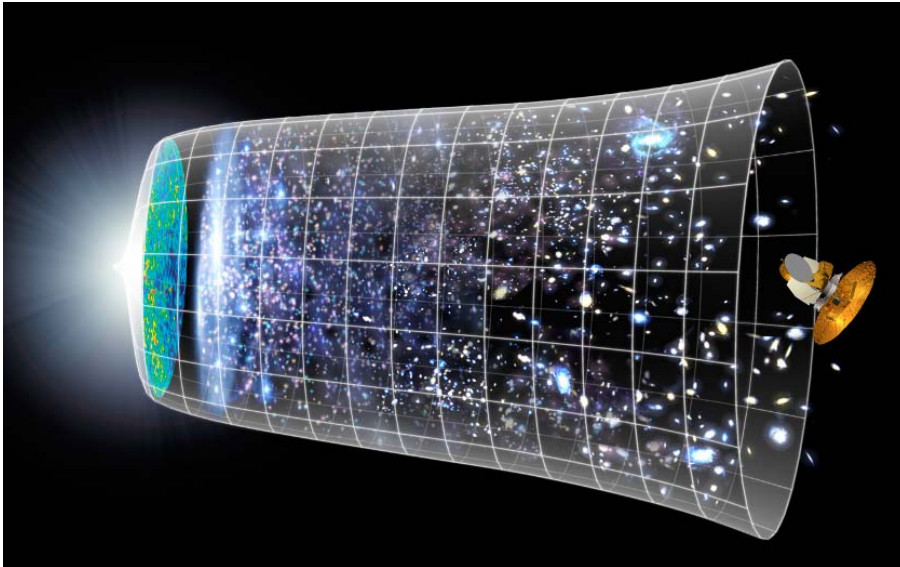
Matter, CDM $w = 0$
Below the scale energy E_c
with $E = m$

$$\rho \propto a^{-3} \leq \rho_c$$

$$v \rightarrow 0$$

Where can find this transition ?

1. As the Universe expands and cools (we go from high to low energy density)
2. Inside Galaxies as we approach the center region (we go from low to high energy density)



CDM or BDM

Substructure Problem (satelites galaxies)

The formation of small structures are surpressed in BDM compared to CDM.

- BDM particles have a dispersion velocity $v = c$, i.e. are HDM, above E_c while they behave as CDM below this scale with $v = 0$.

NO formation of structure for scales smaller than λ_{fs}

$$\lambda_{fs} = a(t) \int_0^t dt' v(t')$$

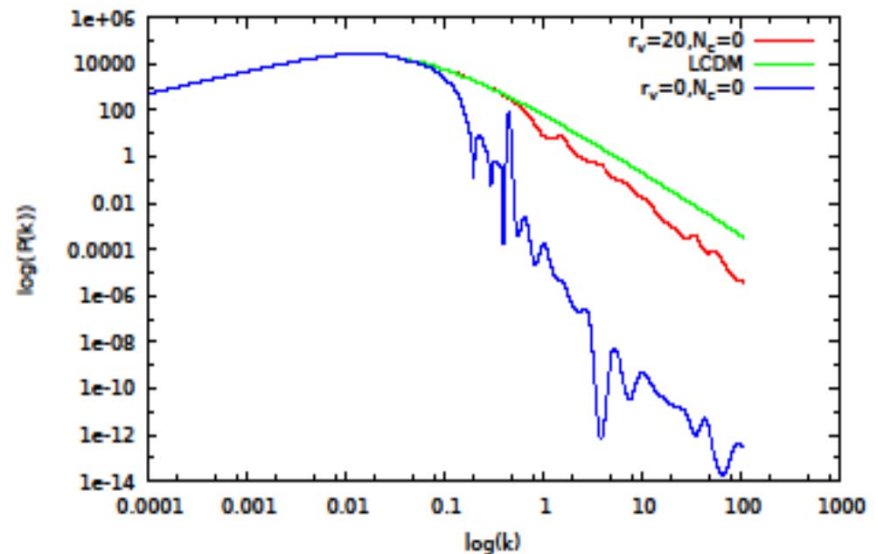
$$\lambda_{fs} = a(t) \int_{a_i}^{a_c} da \frac{v_i}{a^2 H} = \frac{a(t) v_i}{H_c a_c}$$

The observational data requires $\lambda_{fs} < 1 \text{ Mpc}$
giving galaxies with mass $M > 10^9 M_\odot$

Galaxy Mass

$$M_{fs}(E_c) \equiv \frac{4\pi\rho_o}{3} \left(\frac{\lambda_{fs}}{2}\right)^3 =$$

- We obtain a cut off in the power spectrum, due to the free streaming of the particles , λ_{fs} :



CDM or BDM

Rotation Curves => DM profiles

NFW CDM cuspy profile

$$\rho \rightarrow \infty, \quad r \rightarrow 0$$

$$\rho_{NFW} = \frac{\rho_s}{r/r_s(1+r/r_s)^2}$$

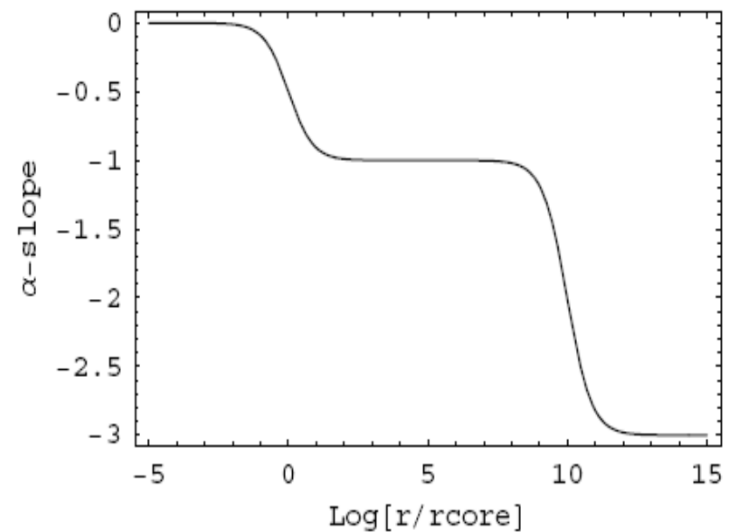
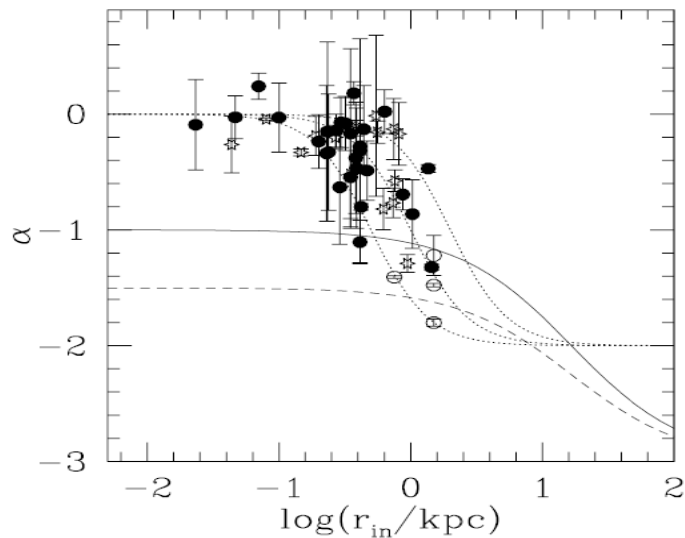
BDM has a core profile

$$\rho \rightarrow cte, \quad r \rightarrow 0$$

$$\rho_{BDM} = \frac{\rho_s}{(r_{core}/r_s + r/r_s)(1+r/r_s)^2}$$

rc size of the core

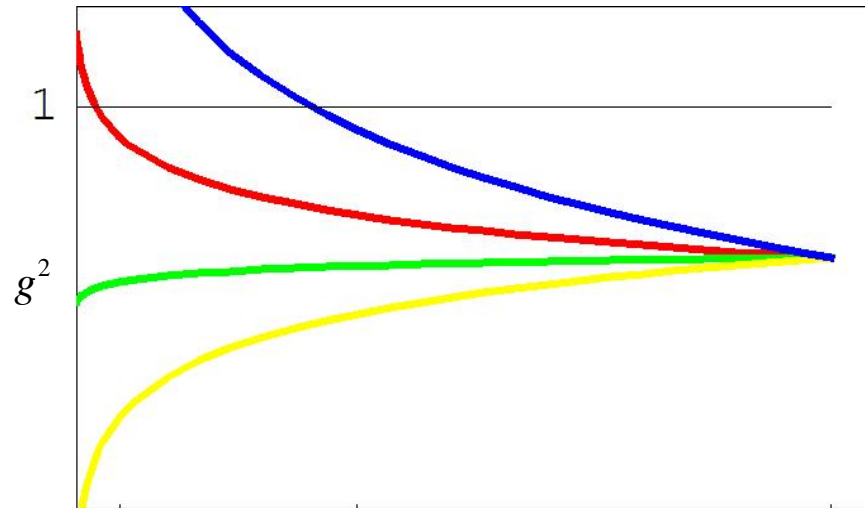
$$\alpha \equiv \frac{d \text{Log}[\rho]}{d \text{Log}[r]}$$



Particle motivation of BDM BOUND DARK MATTER

A.de la M. *Astropart.Phys.* 33:195-200,2010

Evolution of gauge coupling constant vs Energy



$$E_{gut} \cong 10^{16} GeV,$$

$$Log_{10} E$$

SU(3) Interacción Fuerte

SU(N) Dark Matter

SU(2) Interacción Débil

SU(1) E.M. Interac.

- We assume a new Dark Gauge Group with SU(N_c) and N_f number of elementary particles.
- The mass of these elementary particles is small or zero but at low energy a large mass M is generated due to non perturbative physics

One loop Beta-Function evolution

$$\frac{1}{g^2(E)} = \frac{1}{g^2(E_{gut})} + \frac{b}{8\pi^2} \text{Log}\left[\frac{E}{E_{gut}}\right]$$

$$E_{gut} \cong 10^{16} GeV,$$

$$g^2(E_{gut}) \cong 1/2$$

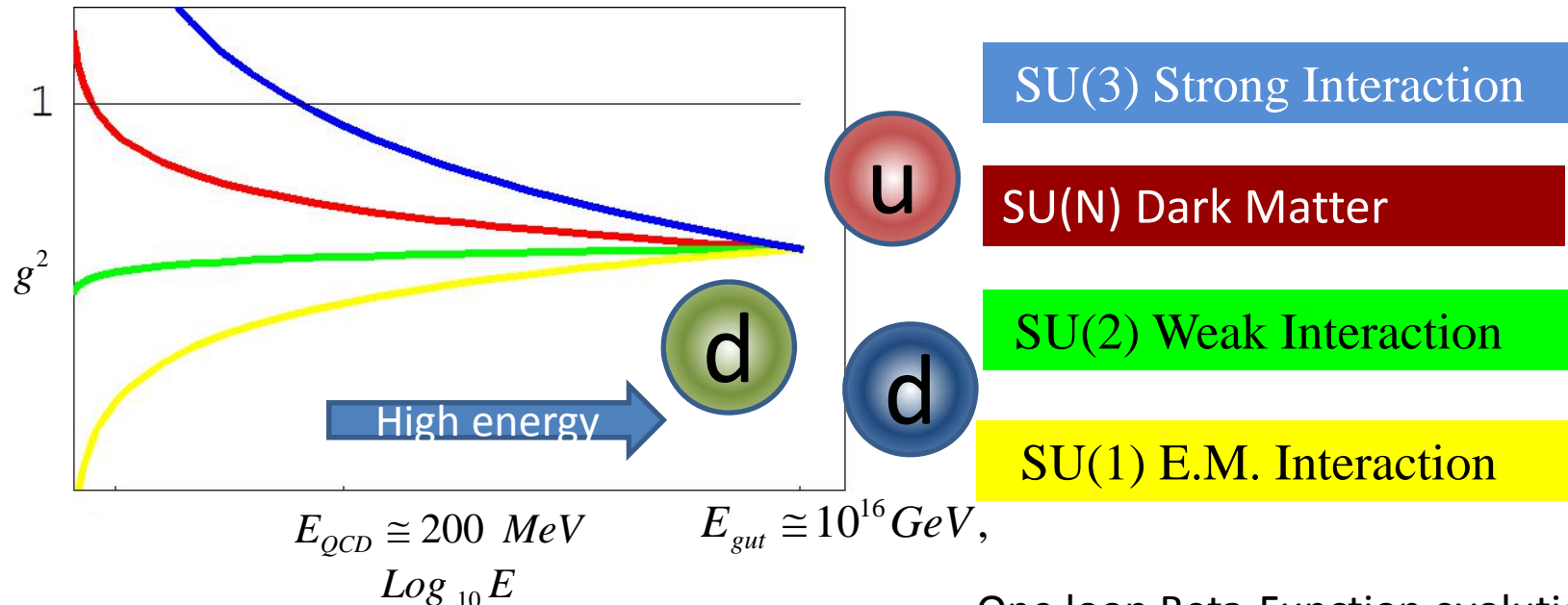
$$b = 3N_c - N_f$$

Particle motivation of BDM

BOUND DARK MATTER

A.de la Macorra, A.de la M Astropart.Phys. 33:195-200,2010

Evolution of gauge coupling constant vs Energy



- We assume a new Dark Gauge Group with $SU(N_c)$ and N_f number of elementary particles.
- The mass of these elementary particles is small or zero but at low energy a large mass M is generated due to non perturbative physics

One loop Beta-Function evolution

$$\frac{1}{g^2(E)} = \frac{1}{g^2(E_{gut})} + \frac{b}{8\pi^2} \text{Log}\left[\frac{E}{E_{gut}}\right]$$

$$E_{gut} \cong 10^{16} \text{ GeV},$$

$$g^2(E_{gut}) \cong 1/2$$

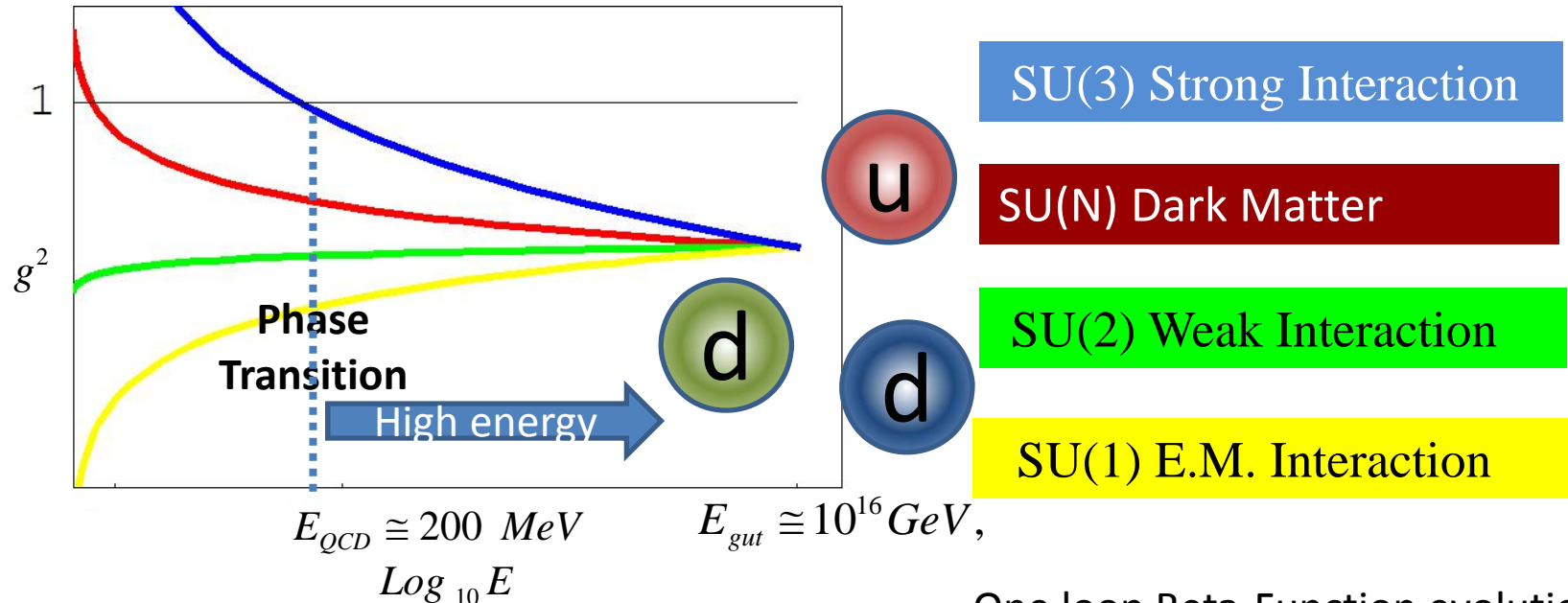
$$b = 3N_c - N_f$$

Particle motivation of BDM

BOUND DARK MATTER

A. de la M. Astropart. Phys. 33:195-200, 2010

Evolution of gauge coupling constant vs Energy



The condensation scale or phase transition scale is defined when the gauge coupling constant becomes strong, i.e.

$$g^2 \gg 1$$

One loop Beta-Function evolution

$$\frac{1}{g^2(E)} = \frac{1}{g^2(E_{gut})} + \frac{b}{8\pi^2} \text{Log}\left[\frac{E}{E_{gut}}\right]$$

$$E_{gut} \cong 10^{16} \text{ GeV},$$

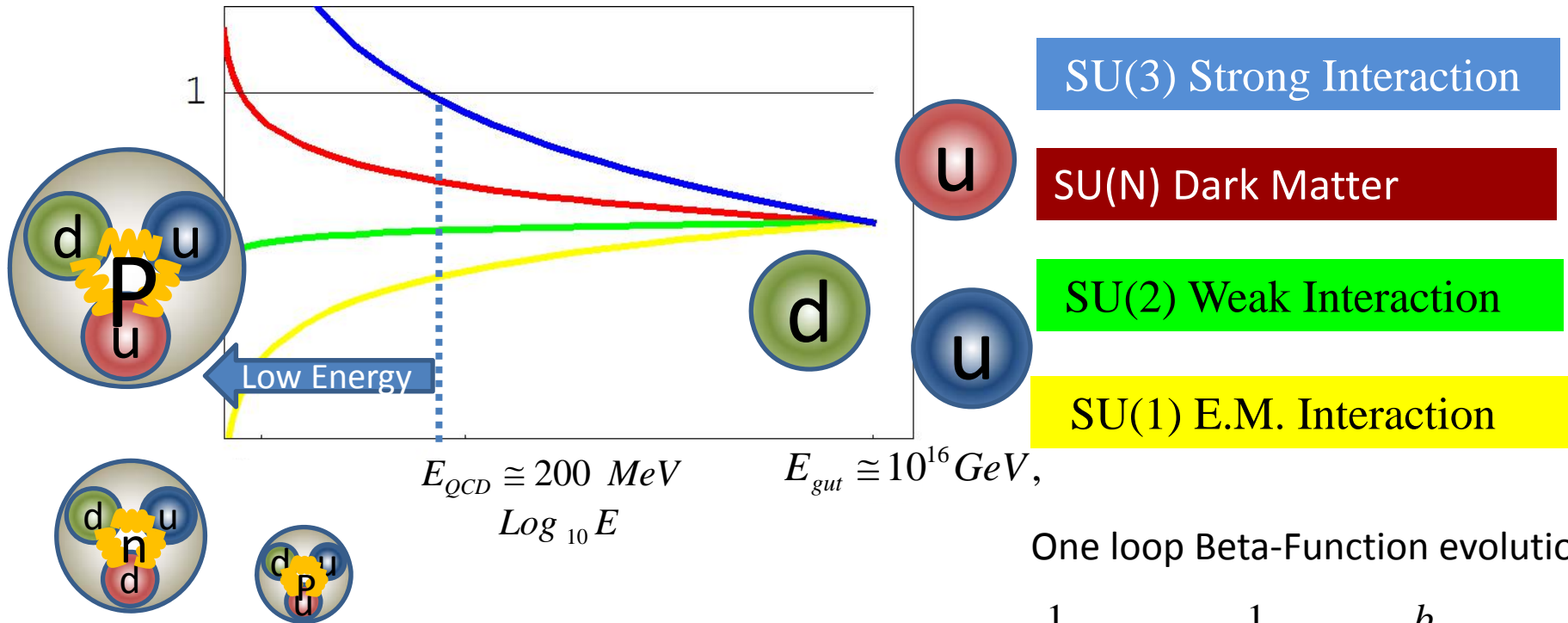
$$g^2(E_{gut}) \cong 1/2$$

$$b = 3N_c - N_f$$

Particle motivation of BDM BOUND DARK MATTER

A. de la M. Astropart. Phys. 33:195-200, 2010

Evolution of gauge coupling constant vs Energy



The value of EQD is determined by gauge dynamics and may be phenomenologically obtained from cosmological data.

One loop Beta-Function evolution

$$\frac{1}{g^2(E)} = \frac{1}{g^2(E_{gut})} + \frac{b}{8\pi^2} \text{Log}\left[\frac{E}{E_{gut}}\right]$$

$$E_{gut} \cong 10^{16} \text{ GeV},$$

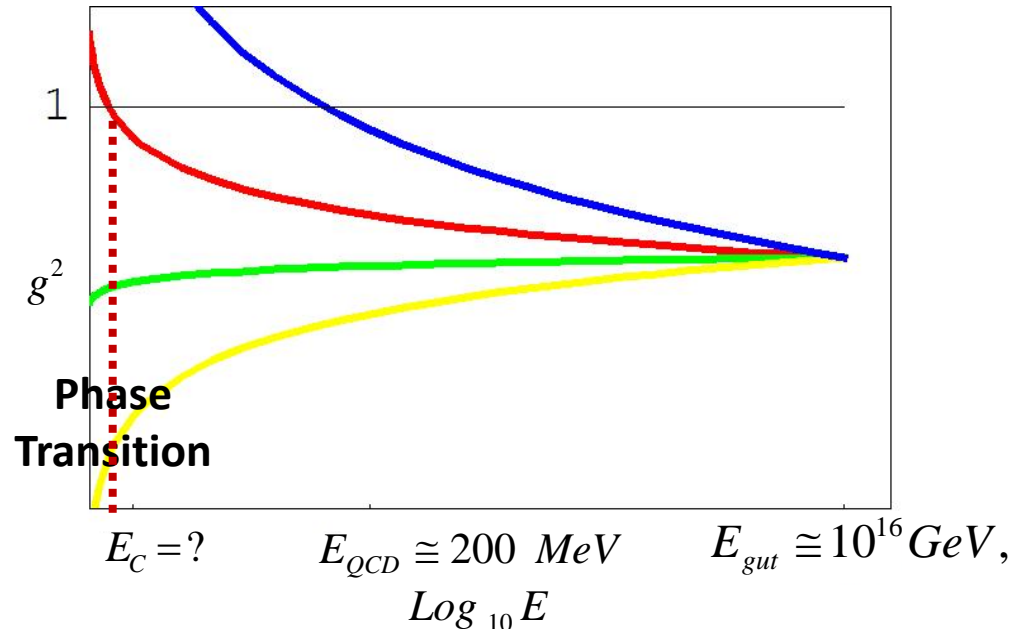
$$g^2(E_{gut}) \cong 1/2$$

$$b = 3N_c - N_f$$

Particle motivation of BDM BOUND DARK MATTER

A. de la M. Astropart. Phys. 33:195-200, 2010

Evolution of gauge coupling constant vs Energy



SU(3) Strong Interaction

SU(N) Dark Matter

SU(2) Weak Interaction

SU(1) E.M. Interaction

The value of E_c is determined by gauge dynamics and may be phenomenologically obtained from cosmological data.

One loop Beta-Function evolution

$$\frac{1}{g^2(E)} = \frac{1}{g^2(E_{gut})} + \frac{b}{8\pi^2} \text{Log}\left[\frac{E}{E_{gut}}\right]$$

$$E_{gut} \cong 10^{16} \text{ GeV},$$

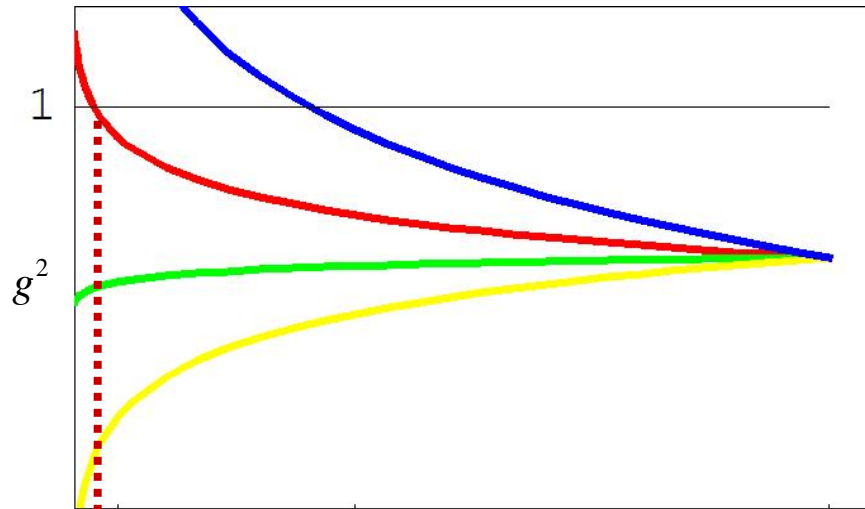
$$g^2(E_{gut}) \cong 1/2$$

$$b = 3N_c - N_f$$

Particle motivation of BDM BOUND DARK MATTER

A. de la M Astropart. Phys. 33:195-200, 2010

Evolution of gauge coupling constant vs Energy



SU(3) Strong Interaction

SU(N) Dark Matter

SU(2) Weak Interaction

SU(1) E.M. Interaction

Phase Transition $E_c = ?$ $E_{QCD} \cong 200 \text{ MeV}$ $E_{gut} \cong 10^{16} \text{ GeV}$,
 $\text{Log}_{10} E$

We expect from gauge group dynamics that the effective mass to be of the order of the phase transition scale E_c

$$E_c = E_i e^{-8\pi^2/bg_i}$$

$$m_{bdm} = k E_c$$

$$k \approx O(1-10)$$

e.g. proton $m = 938$ with

$E_{QCD} = 200 \text{ MeV}$, $c = 4.6$

One loop Beta-Function evolution

$$\frac{1}{g^2(E)} = \frac{1}{g^2(E_{gut})} + \frac{b}{8\pi^2} \text{Log}\left[\frac{E}{E_{gut}}\right]$$

$$E_{gut} \cong 10^{16} \text{ GeV},$$

$$g^2(E_{gut}) \cong 1/2$$

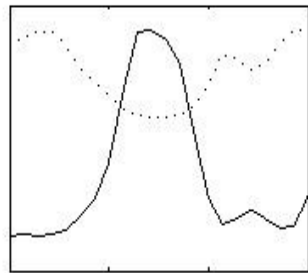
$$b = 3N_c - N_f$$

Linear Evolution of energy density perturbations

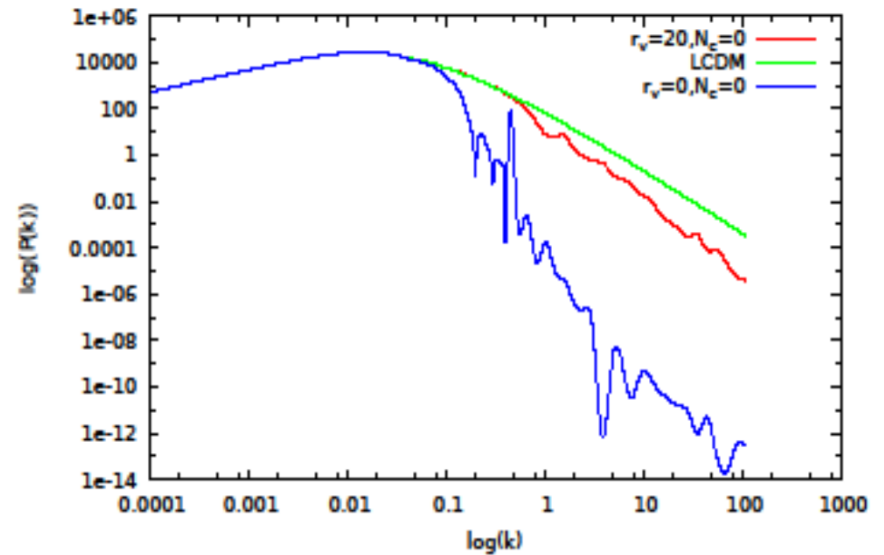
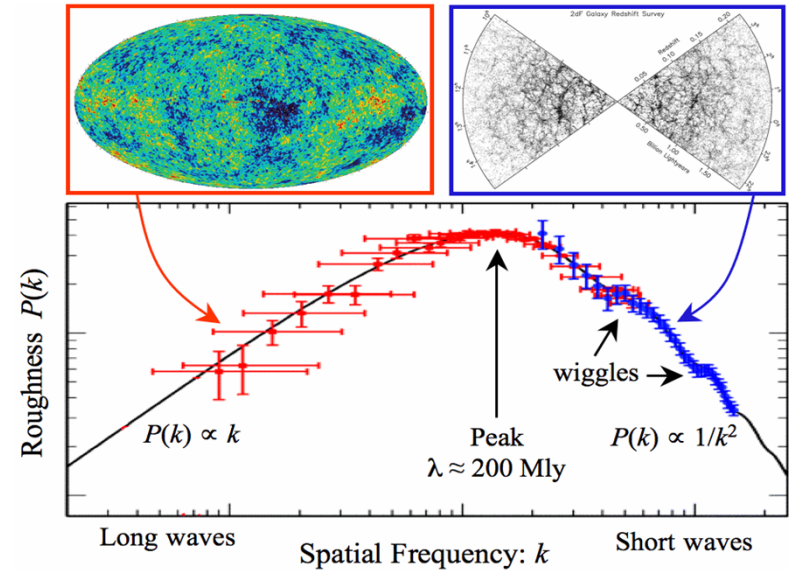
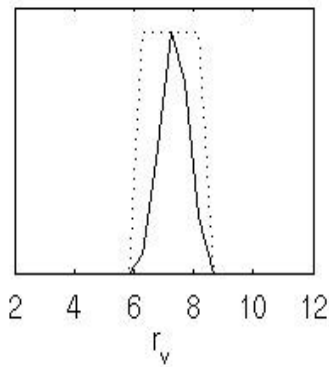
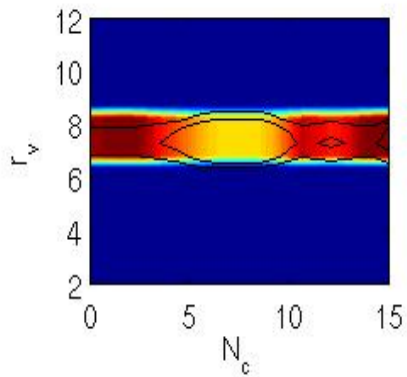
$$w = \frac{p}{\rho} = \frac{v^2}{3}$$

$$v = 1 \quad a < a_c$$

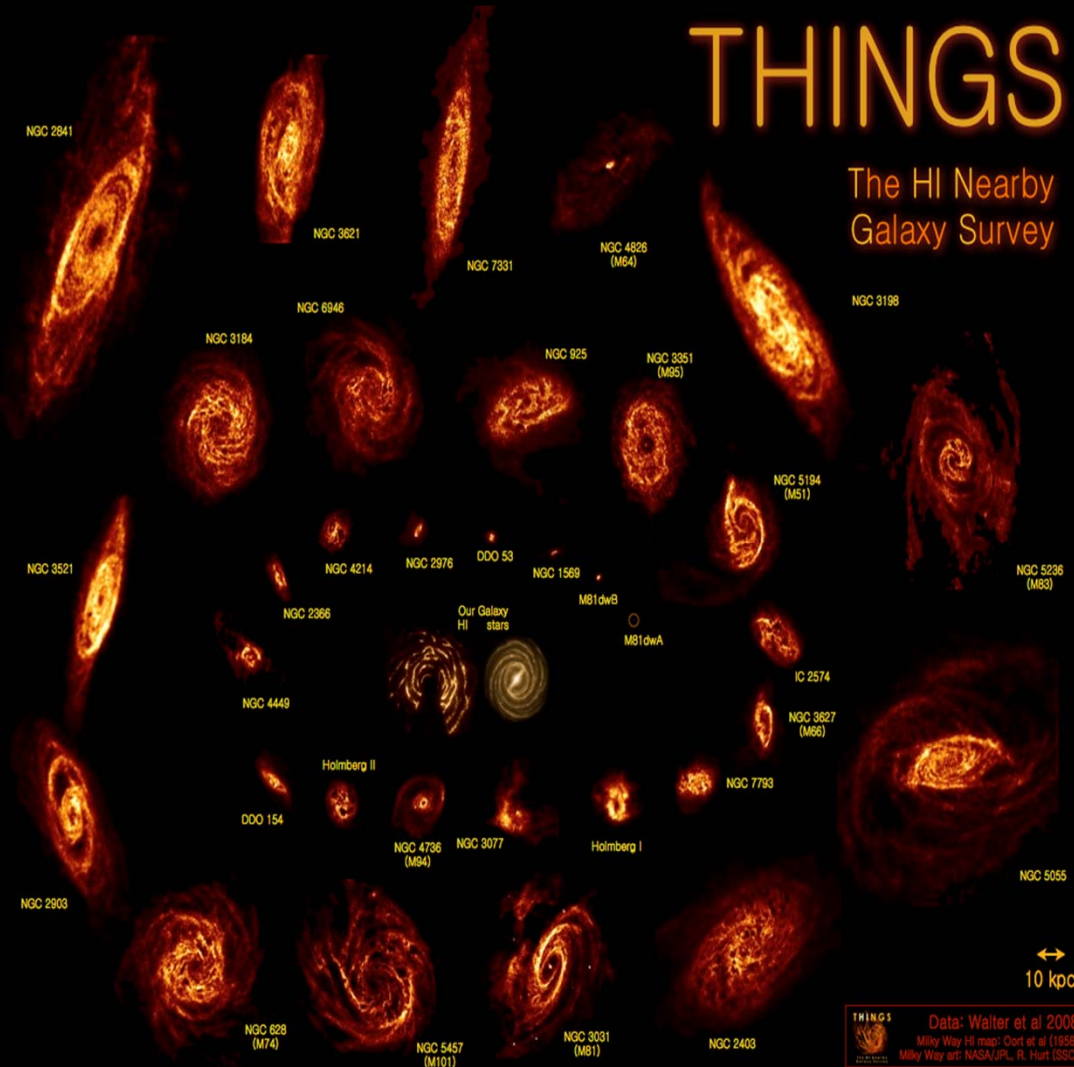
$$v = v_i \left(\frac{a_c}{a} \right) \quad a \geq a_c$$



$$a_c = a_{eq} e^{-N_c}, \quad v_i = e^{-r_v}$$



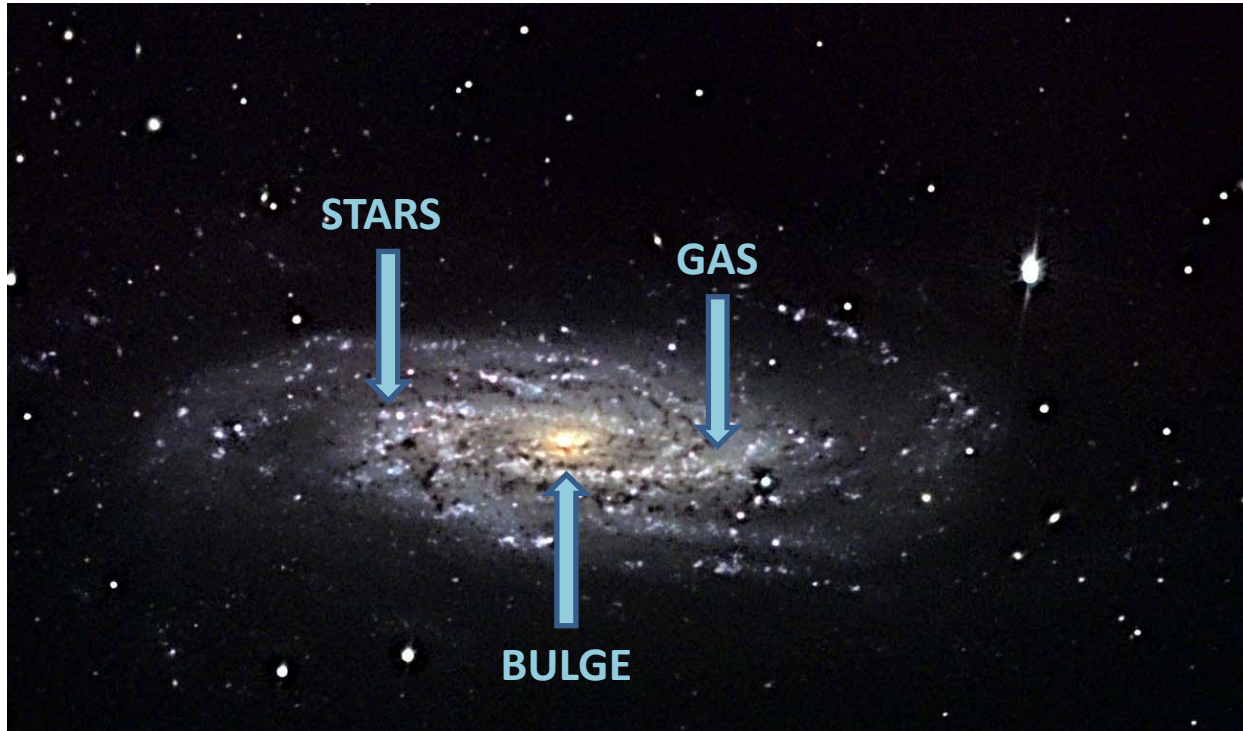
SAMPLE: THINGS (34 High resolution Nearby Galaxies)



- We limit our sample to 17 low luminous (early type and dwarf) galaxies with smooth, symmetric and extended to large radii rotation curves and small or none bulge.
- These properties provide a good estimate of the DM halo in galaxies because it is believed that it dominates over all other components at all radii.
- Great angular resolution in sub kpc

MASS MODEL

Matter Components

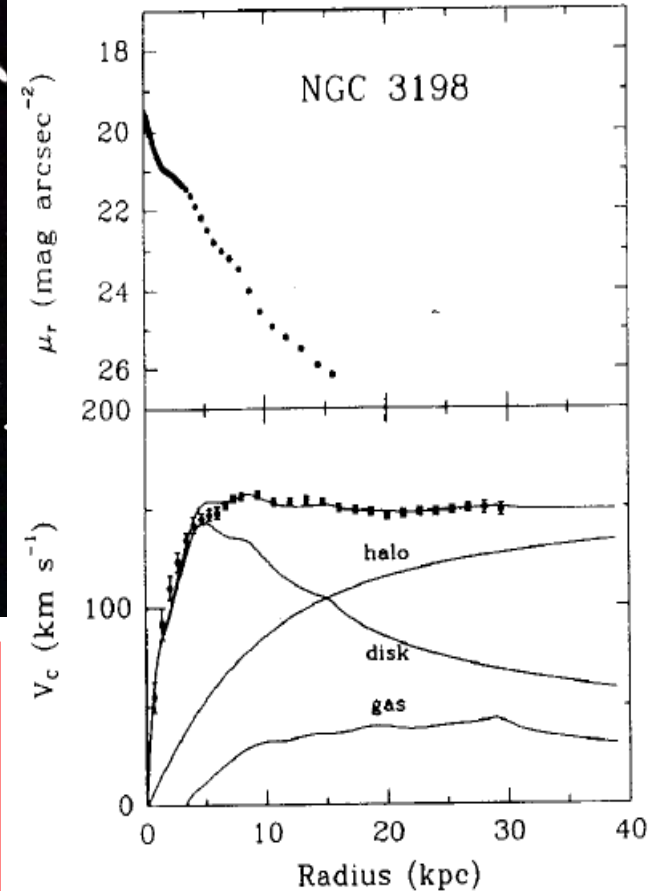


Visible matter components

- Stars
- Bulb
- Gas

Rotation curves also require extra matter:

- Dark Matter



MASS MODEL

Halo Profile : NFW

Cuspy

$$\rho_{NFW} = \frac{\rho_0}{\frac{r}{r_s} \left(1 + \frac{r}{r_s}\right)^2}$$

Halo Profile : BDM

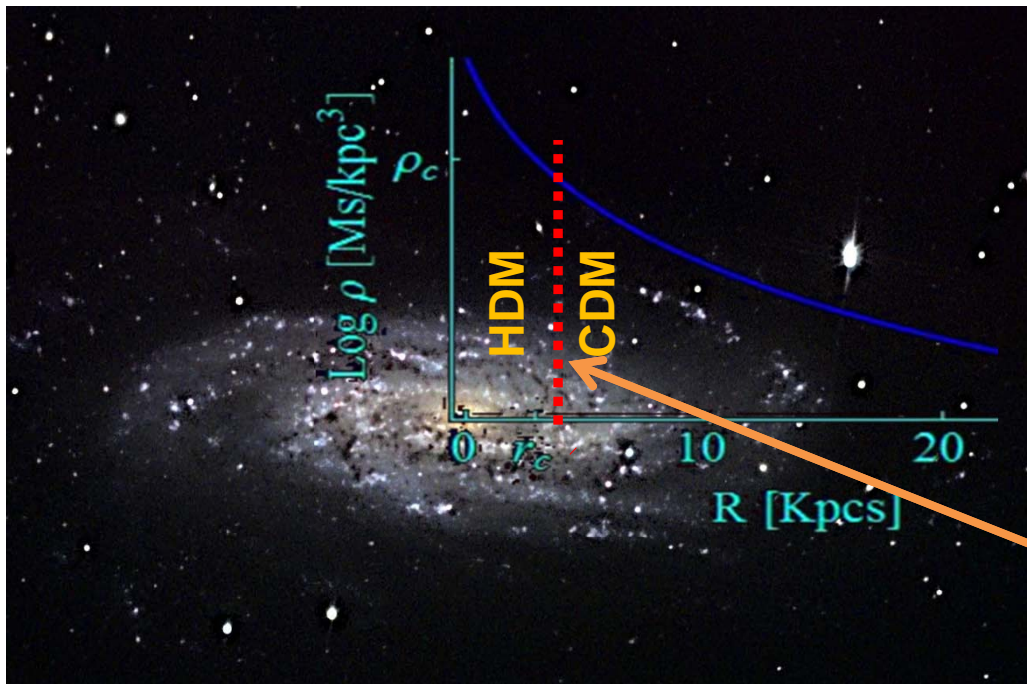
Core

$$\rho_{BDM} = \frac{\rho_0}{\left(\frac{r_c}{r_s} + \frac{r}{r_s}\right) \left(1 + \frac{r}{r_s}\right)^2}$$

BDM gives a core for
 $\rho_g > \rho_c = E c^4$

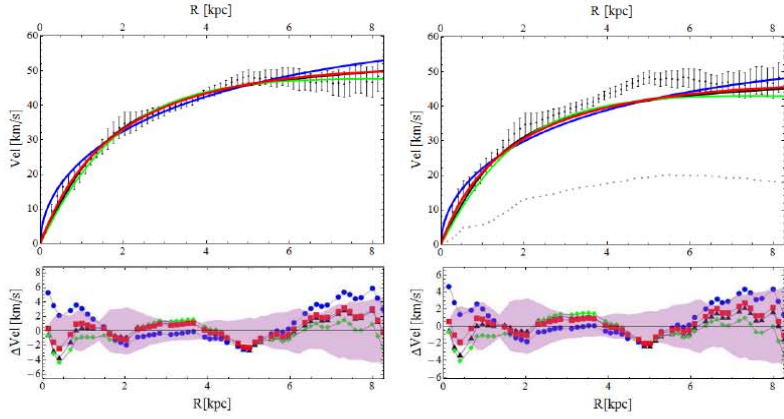
$$E c^4 = \rho_{BDM}(r=r_c) \equiv \rho_c$$

$$\rho_c = \frac{\rho_0 r_s}{2 r_c}$$



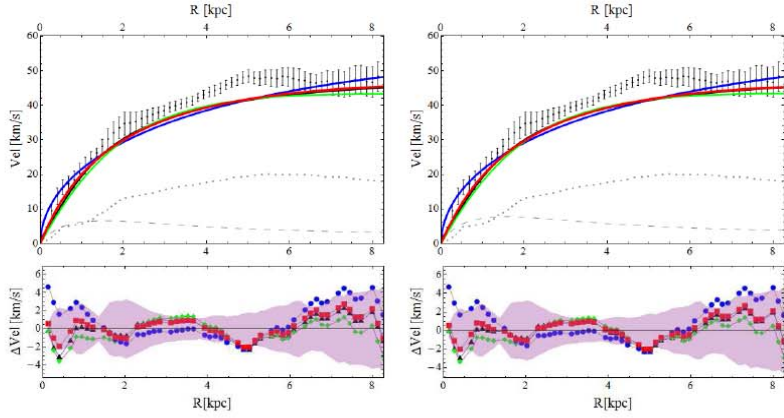
A large number of galaxies dominated by DM, as Dwarf galaxies or LSB (Low Surface Brightness), have a better fit to rotation curves with a core DM profile instead as the CDM NFW cuspy profile.

Phase transition from CDM to HDM



(a) Minimal disk

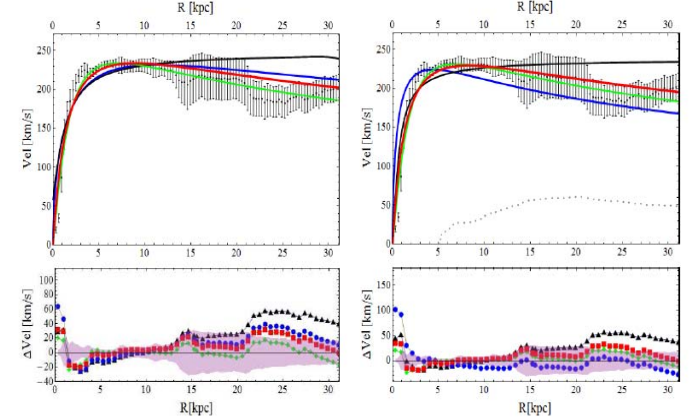
(b) Min. disk + Gas



(c) Kroupa

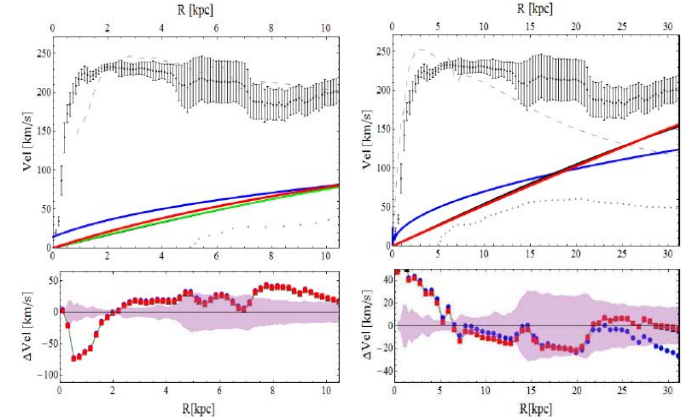
(d) diet-Salpeter

FIG. 10: Graphical visualization of the rotation curves for the galaxies DDO 154 belonging to the group G. where $r_c < r_s$ for all mass models. Is a dwarf galaxy, one of the first galaxies used to illustrate the conflict with the theoretical prediction of the Λ CDM [17]. No significant color gradient in the colors (B-V) and (B-I) is detected, constant color as function of radius in our models is well assumed with the value for $\Upsilon_* = 0.5$. For a single exponential disk we use value of $\mu_0 = 20.8 \text{ mag arcsec}^{-2}$ and $R_d = 0.72 \text{ kpc}$. BDM is the best option since it predict a value of Υ_* very close to the minimal disk and gives the best fit. The values for r_s and r_c are very reasonable except when we considered the Kroupa IMF. From left to right and top to bottom, images from the fit considering minimal disk, minimal disk+gas, Kroupa, diet-Salpeter. In the top images of each galaxy are represent the four DM profiles: BDM, red squares; NFW, blue circles; Burkert, green diamond; Isothermal, black triangles. The dotted line is the gas component, the short dashed line is the stellar contribution and the tick points are the observational data with its respectively error bars. At the bottom images we plot the difference between the observed and predicted curves where the purple region represents the error of the observations and each different line represent the fitted curve of the different profiles with the observations taking into account already all the mass contributions.



(a) Minimal disk

(b) Min. disk + Gas



(c) Kroupa

(d) diet-Salpeter

FIG. 22: The rotation curves for the galaxy NGC 3521. Colors and symbols are as in Fig.10. Because the nature of the galaxy it is difficult to obtain reliable data from the stellar component (see deBlok08). even so, we treat the stellar disk as a single component with mass $M_* = 1.2 * 10^{11} M_\odot$ and $R_d = 3 \text{ kpc}$. A color gradient is present. The inner analysis is carried out with data below the 3.7 kpc and obtaining values for the core and central density $r_c = 2.4 \text{ kpc}$ and $r_s = 5.5 \text{ kpc}$ and $\rho_0 = 2.4 * 10^8 M_\odot/\text{kpc}^3$ for the minimal disk.

MINIMUM DISK												
Galaxy (1)	r_c/r_s (2)	BDM				NFW				Fixed-BDM $E_c = 0.11$		
		r_s (3)	$\log_{10} \rho_0$ (4)	r_c (5)	χ^2_{red} (6)	r_s (7)	$\log_{10} \rho_0$ (8)	χ^2_{red} (9)	r_s (10)	r_c (11)	χ^2_{red} (12)	
DDO154	0.37	$3.66^{+0.03}_{-0.03}$	$7.35^{+5.44}_{-5.44}$	$1.35^{+0.04}_{-0.04}$	0.38	$14.46^{+0.14}_{-0.14}$	$6.21^{+4.31}_{-4.3}$	1.48	$12.39^{+0.44}_{-0.44}$	$0.02^{+0.002}_{-0.002}$	1.17	
NGC2841	10^{-5}	$4.67^{+0.01}_{-0.01}$	$8.61^{+6.33}_{-6.11}$	$0.0001^{+0.01}_{-0.01}$	0.58	$4.67^{+0.01}_{-0.01}$	$8.61^{+6.33}_{-6.13}$	0.58	$2.59^{+0.02}_{-0.02}$	$1.87^{+0.005}_{-0.005}$	0.80	
G.A NGC3031	0.12	$1.55^{+0.003}_{-0.003}$	$9.38^{+7.01}_{-7.01}$	$0.19^{+0.01}_{-0.01}$	4.24	$1.86^{+0.004}_{-0.004}$	$9.17^{+6.79}_{-6.79}$	4.20	$0.69^{+0.02}_{-0.02}$	$1.62^{+0.003}_{-0.003}$	4.21	
NGC3621	0.01	$7.79^{+0.02}_{-0.02}$	$7.5^{+5.21}_{-5.21}$	$0.01^{+0.01}_{-0.01}$	2.04	$7.9^{+0.02}_{-0.02}$	$7.49^{+5.19}_{-5.21}$	2.02	$6.53^{+0.04}_{-0.04}$	$0.29^{+0.001}_{-0.001}$	2.38	
NGC4736	0.18	$0.27^{+0.001}_{-0.001}$	$10.71^{+8.61}_{-8.61}$	$0.05^{+0.01}_{-0.01}$	1.69	$0.33^{+0.001}_{-0.001}$	$10.47^{+8.36}_{-8.36}$	1.67	$0.02^{+0.001}_{-0.001}$	$1.06^{+0.003}_{-0.003}$	1.72	
NGC6946	0.02	$5.95^{+0.01}_{-0.01}$	$8.01^{+5.64}_{-5.64}$	$0.12^{+0.02}_{-0.02}$	1.37	$6.61^{+0.02}_{-0.02}$	$7.9^{+5.54}_{-5.54}$	1.38	$4.33^{+0.03}_{-0.03}$	$0.7^{+0.003}_{-0.003}$	1.42	
NGC7793	0.01	$7.21^{+0.05}_{-0.05}$	$7.41^{+5.39}_{-5.39}$	$0.06^{+0.01}_{-0.01}$	3.69	$8.68^{+0.06}_{-0.06}$	$7.27^{+5.25}_{-5.25}$	3.75	$5.4^{+0.1}_{-0.1}$	$0.22^{+0.002}_{-0.002}$	3.80	
IC2574	1	$17.27^{+0.17}_{-0.16}$	$7^{+5.16}_{-1.24}$	$18.28^{+0.34}_{-0.38}$	0.43	$\sim 10^4$	$2.85^{+1.03}_{-1.01}$	6.17	$> 10^6$	$0.02^{+0.001}_{-0.001}$	5.49	
NGC2366	1	$2.25^{+0.00001}_{-0.00001}$	$7.96^{+6.52}_{-6.4}$	$2.25^{+0.001}_{-0.001}$	2.11	$18.62^{+0.48}_{-0.47}$	$6.15^{+4.65}_{-4.65}$	4.45	$11.68^{+1.03}_{-1.03}$	$0.03^{+0.001}_{-0.001}$	3.98	
NGC2903	1	$1.90^{+0.002}_{-0.002}$	$9.26^{+7.07}_{-7.00}$	$1.90^{+0.02}_{-0.02}$	1.72	$3.91^{+0.01}_{-0.01}$	$8.38^{+6.19}_{-6.12}$	2.36	$2.44^{+0.02}_{-0.02}$	$1.04^{+0.004}_{-0.004}$	1.75	
G.B NGC2976	1	$2.53^{+0.001}_{-0.001}$	$8.5^{+6.6}_{-6.85}$	$2.53^{+0.001}_{-0.001}$	0.69	$\sim 10^4$	$3.27^{+1.5}_{-1.5}$	2.86	$> 10^6$	$0.12^{+0.001}_{-0.001}$	1.23	
NGC3198	1	$3.76^{+0.01}_{-0.01}$	$8.41^{+6.18}_{-6.22}$	$3.76^{+0.06}_{-0.06}$	0.59	$9.02^{+0.03}_{-0.03}$	$7.39^{+5.16}_{-5.21}$	1.80	$7.85^{+0.05}_{-0.05}$	$0.25^{+0.001}_{-0.001}$	1.23	
NGC3521	1	$2.00^{+0.0001}_{-0.0001}$	$9.31^{+7.47}_{-7.08}$	$2.00^{+0.001}_{-0.001}$	1.37	$5.25^{+0.03}_{-0.03}$	$8.22^{+6.19}_{-6.19}$	7.17	$2.43^{+0.04}_{-0.04}$	$1.22^{+0.008}_{-0.008}$	2.72	
NGC925	1	$10.36^{+0.08}_{-0.08}$	$7.53^{+5.6}_{-5.65}$	$12.18^{+0.23}_{-0.23}$	0.31	$\sim 10^4$	$2.27^{+0.39}_{-0.39}$	1.46	$> 10^7$	$0.04^{+0.001}_{-0.001}$	1.32	
NGC2403	$< 10^{-6}$	$6.94^{+0.01}_{-0.01}$	$7.51^{+5.11}_{-5.11}$	< 0.01	0.79	$6.94^{+0.01}_{-0.01}$	$7.51^{+5.11}_{-5.11}$	0.79	$5.59^{+0.02}_{-0.02}$	$0.27^{+0.001}_{-0.001}$	1.24	
G.C NGC5055	$< 10^{-6}$	$4.03^{+0.01}_{-0.01}$	$8.38^{+6.05}_{-6.05}$	< 0.01	1.38	$4.03^{+0.01}_{-0.01}$	$8.38^{+6.05}_{-6.05}$	1.37	$2.27^{+0.02}_{-0.02}$	$1.13^{+0.004}_{-0.004}$	2.90	
NGC7331	$< 10^{-6}$	$3.56^{+0.01}_{-0.01}$	$8.67^{+6.5}_{-6.5}$	< 0.01	0.85	$3.56^{+0.01}_{-0.01}$	$8.67^{+6.5}_{-6.5}$	0.85	$1.83^{+0.02}_{-0.02}$	$1.58^{+0.006}_{-0.006}$	1.03	

BDM Profile

$$\rho_{\text{BDM}} = \frac{\rho_0}{\left(\frac{r_c}{r_s} + \frac{r}{r_s}\right) \left(1 + \frac{r}{r_s}\right)^2}$$

TABLE II: We present the results discussed in Sec. VI for BDM (Eq. (5)) with its three free parameters (r_c , r_s , and ρ_0) and the NFW (Eq. (11)) profiles with the minimal disk model. Also, in the last three columns, we present the result obtained with the BDM profiles fixing the value of E_c to 0.11 eV as explained in Sec. VIC. Column (2) shows the ratio between the core radius r_c and the scale distance r_s , and galaxies are grouped by de value of this quotient. Columns (3-6) are the fitted results when only DM and the BDM profile are considered in the mass model. (7-9) show the results for NFW with the same mass model. In (10-12) we show the results for the fixed BDM model. All distance scales such as r_c and r_s are given in kpc. Logarithm base 10 of the densities ρ_0 is given in M_\odot/kpc^3 . (6,9,12) show the value of χ^2 is normalized to the numbers of data points minus the number of free parameter.

KROUPA											
Galaxy (1)	r_c/r_s (2)	BDM				NFW			Fixed-BDM $E_c = 0.06$		
		r_s (3)	$\log_{10} \rho_0$ (4)	r_c (5)	χ^2_{red} (6)	r_s (7)	$\log_{10} \rho_0$ (8)	χ^2_{red} (9)	r_s (10)	r_c (11)	χ^2_{red} (12)
DDO154	0.23	$4.37^{+0.04}_{-0.04}$	$7.08^{+5.27}_{-5.26}$	$0.99^{+0.05}_{-0.05}$	0.28	$15.14^{+0.17}_{-0.15}$	$6.1^{+4.28}_{-4.28}$	1.06	$7.3^{+0.25}_{-0.25}$	$0.31^{+0.}_{-0.}$	0.35
NGC2841	$< 10^{-6}$	$6.67^{+0.02}_{-0.02}$	$8.18^{+5.89}_{-5.89}$	< 0.01	1.3	$6.67^{+0.02}_{-0.02}$	$8.18^{+5.89}_{-5.89}$	1.29	$3.16^{+0.11}_{-0.11}$	$5.97^{+0.02}_{-0.02}$	1.21
G.A NGC3031	$< 10^{-6}$	$8.35^{+0.06}_{-0.06}$	$7.48^{+5.56}_{-5.55}$	< 0.03	5.01	$8.35^{+0.06}_{-0.06}$	$7.48^{+5.56}_{-5.55}$	4.96	$3.09^{+0.21}_{-0.21}$	$3.2^{+0.02}_{-0.02}$	5.02
NGC3621	$< 10^{-6}$	$17.1^{+0.08}_{-0.08}$	$6.72^{+4.6}_{-4.6}$	< 0.01	1.46	$17.1^{+0.08}_{-0.08}$	$6.72^{+4.6}_{-4.6}$	1.45	$20.3^{+0.27}_{-0.27}$	$0.90^{+0.01}_{-0.01}$	1.72
NGC4736	1.05	$0.13^{+0.02}_{-0.01}$	$11.19^{+9.49}_{-9.49}$	$0.14^{+0.02}_{-0.01}$	1.34	$0.23^{+0.02}_{-0.02}$	$10.44^{+8.74}_{-8.74}$	1.34	< 0.01	$1.90^{+0.02}_{-0.02}$	1.65
NGC6946	0.03	$35.13^{+0.24}_{-0.27}$	$6.49^{+4.49}_{-4.49}$	$1.17^{+0.07}_{-0.07}$	1.13	$96.74^{+0.84}_{-0.85}$	$5.87^{+3.87}_{-3.87}$	1.21	$31.3^{+0.98}_{-0.98}$	$1.20^{+0.01}_{-0.01}$	1.13
NGC7793	$< 10^{-6}$	$8.62^{+0.08}_{-0.08}$	$7.15^{+5.26}_{-5.25}$	< 0.01	4.13	$8.62^{+0.08}_{-0.08}$	$7.15^{+5.26}_{-5.25}$	4.07	$40.9^{+8.20}_{-8.20}$	$0.65^{+0.02}_{-0.02}$	31.1
IC2574	0.32	$48.39^{+0.88}_{-0.89}$	$6.14^{+4.5}_{-4.51}$	$15.61^{+0.49}_{-0.46}$	0.75	$> 10^6$	$0.1^{+1.62}_{-1.46}$	2.4	$23.0^{+1.20}_{-1.20}$	< 0.01	-
NGC2366	1	$2.03^{+0.30}_{-0.30}$	$7.87^{+5.90}_{-5.90}$	$2.03^{+0.2}_{-0.2}$	1.71	$15.5^{+1.1}_{-1.1}$	$6.07^{+4.81}_{-4.81}$	3	$9.02^{+0.80}_{-0.80}$	$0.28^{+0.01}_{-0.01}$	2.22
NGC2903	1	$2.34^{+0.18}_{-0.15}$	$9.02^{+6.97}_{-6.7}$	$2.35^{+0.03}_{-0.03}$	2.13	$4.92^{+0.02}_{-0.02}$	$8.12^{+5.94}_{-5.94}$	3.43	$1.67^{+0.07}_{-0.07}$	$4.36^{+0.01}_{-0.01}$	2.67
G.B NGC2976	0.8	$40.2^{+2.10}_{-2.10}$	$7.61^{+5.80}_{-5.71}$	$29.9^{+2.10}_{-2.10}$	1.28	$> 10^5$	< 2	6.31	$> 10^5$	$4.28^{+0.31}_{-0.36}$	4.33
NGC3198	0.9	$8.28^{+0.03}_{-0.03}$	$7.58^{+5.53}_{-5.53}$	$8.27^{+0.18}_{-0.17}$	3.51	$24.2^{+0.13}_{-0.13}$	$6.42^{+4.37}_{-4.37}$	4.99	$17.2^{+0.21}_{-0.21}$	$0.93^{+0.01}_{-0.01}$	4.1
NGC3521	0.06	$128^{+5.21}_{-5.67}$	$5.65^{+4.44}_{-4.36}$	$7.58^{+1.09}_{-0.98}$	5.74	$> 10^6$	$1.01^{+0.24}_{-0.24}$	9.26	$> 10^7$	$0.29^{+0.01}_{-0.01}$	9.01
NGC925	1	$48.56^{+0.8}_{-0.83}$	$6.77^{+5.1}_{-5.15}$	$48.56^{+1.39}_{-0.26}$	1.24	$> 10^5$	$1.95^{+0.34}_{-0.32}$	3.68	$> 10^7$	$0.21^{+0.01}_{-0.01}$	22.2
NGC2403	0.004	$10.45^{+0.03}_{-0.03}$	$7.14^{+4.87}_{-4.72}$	$0.05^{+0.01}_{-0.01}$	0.8	$10.38^{+0.03}_{-0.03}$	$7.14^{+4.79}_{-4.8}$	0.82	$4.36^{+0.04}_{-0.04}$	$2.29^{+0.01}_{-0.01}$	0.98
G.C NGC5055	0.4	$45.9^{+0.39}_{-0.48}$	$6.31^{+4.50}_{-4.50}$	$18.24^{+0.59}_{-0.76}$	4.35	$> 10^6$	< 2	5.09	$> 10^3$	$0.25^{+0.01}_{-0.01}$	5.00
NGC7331	0	$> 10^5$	$2.11^{+0.22}_{-0.21}$	$3.76^{+0.2}_{-0.19}$	7.92	$> 10^6$	< 2	8.63	580^{+127}_{-127}	$0.94^{+0.01}_{-0.01}$	8.14

TABLE IV: This table show the fitted values when considering the Kroupa IMF for the value of the stellar disk, columns (2-6) show the BDM and columns (7-9) NFW parameters. Columns (10-12) are the parameters obtained with the BDM profile by fixing $E_c = 0.05$ eV, cf. VIA . Units and the set of galaxies are as show in Table.II.

NFW Profile

$$\rho_{\text{NFW}} = \frac{\rho_0}{\frac{r}{r_s} \left(1 + \frac{r}{r_s}\right)^2}$$

(1 σ , 2 σ) 2-D contour plots of ρ_0 vs r_c core for diff. Mass models

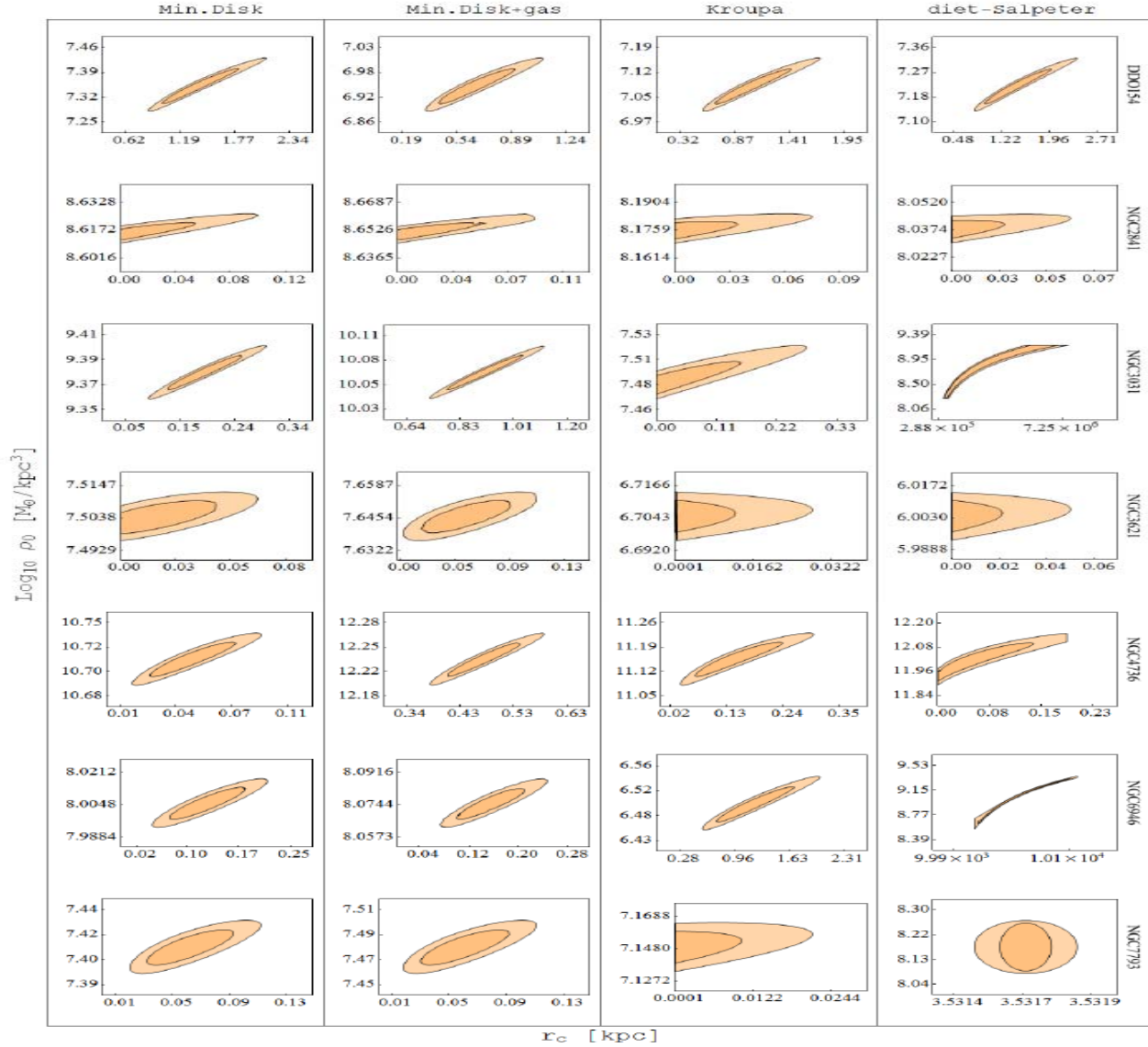


FIG. 2: We present the 2D likelihood contours for the BDM parameters ρ_0 and r_c for galaxies with $r_c \ll r_s$, group A. The two regions in each figure correspond to 1 σ (68%) and 2 σ (95%) confidence level. Columns from left to right correspond to minimal disk, minimal disk + gas, Kroupa and diet-Salpeter mass models. This clearly shows how the stars has an important contribution close to the center of the galaxy and erase trace of the core, we can see that even if the value of r_c that minimize χ^2 is zero, is consistent with values different from zero up to 1 σ .

(1 σ , 2 σ) 2-D contour plots of ρ_0 vs r_c core for diff. Mass models

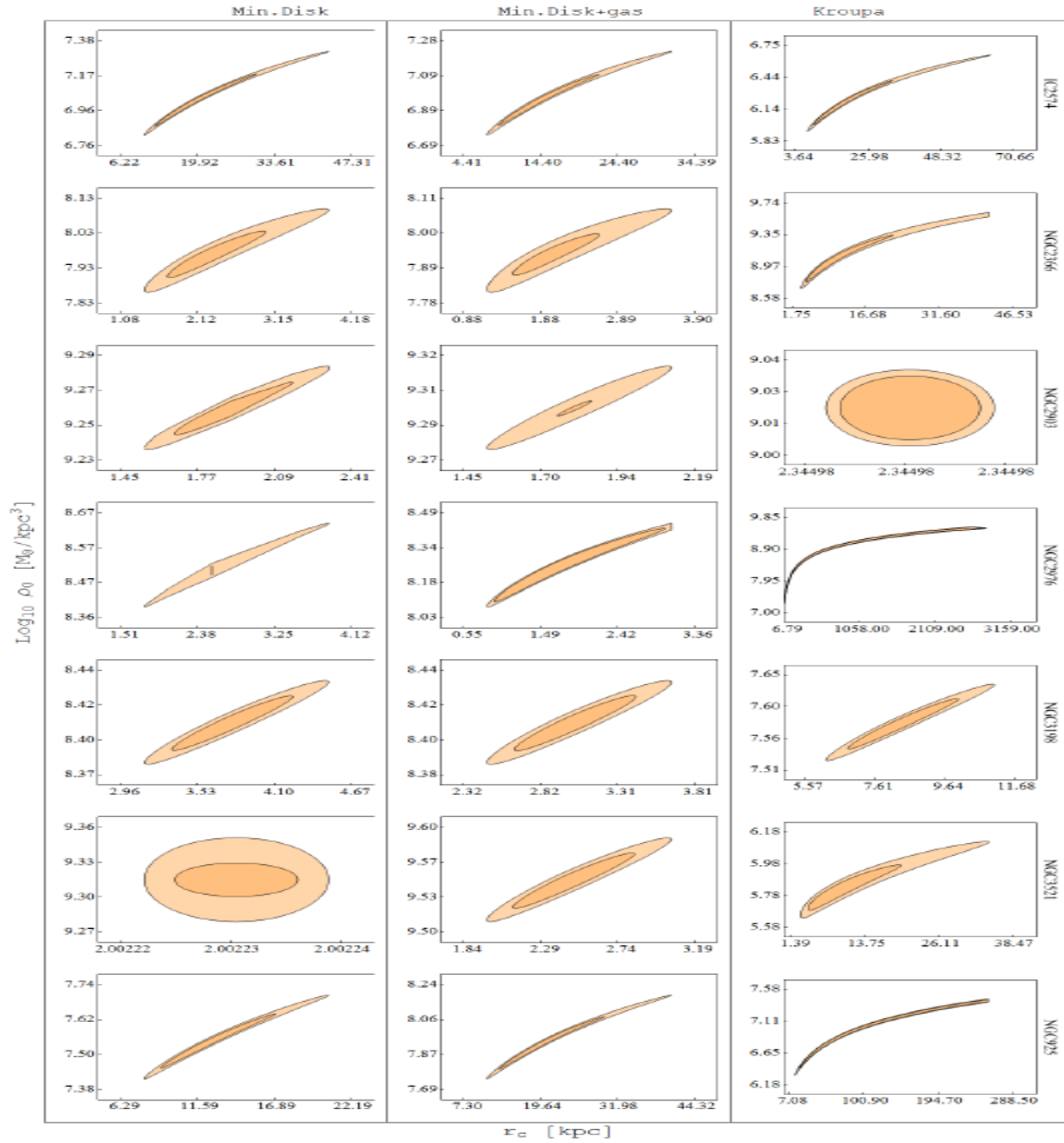
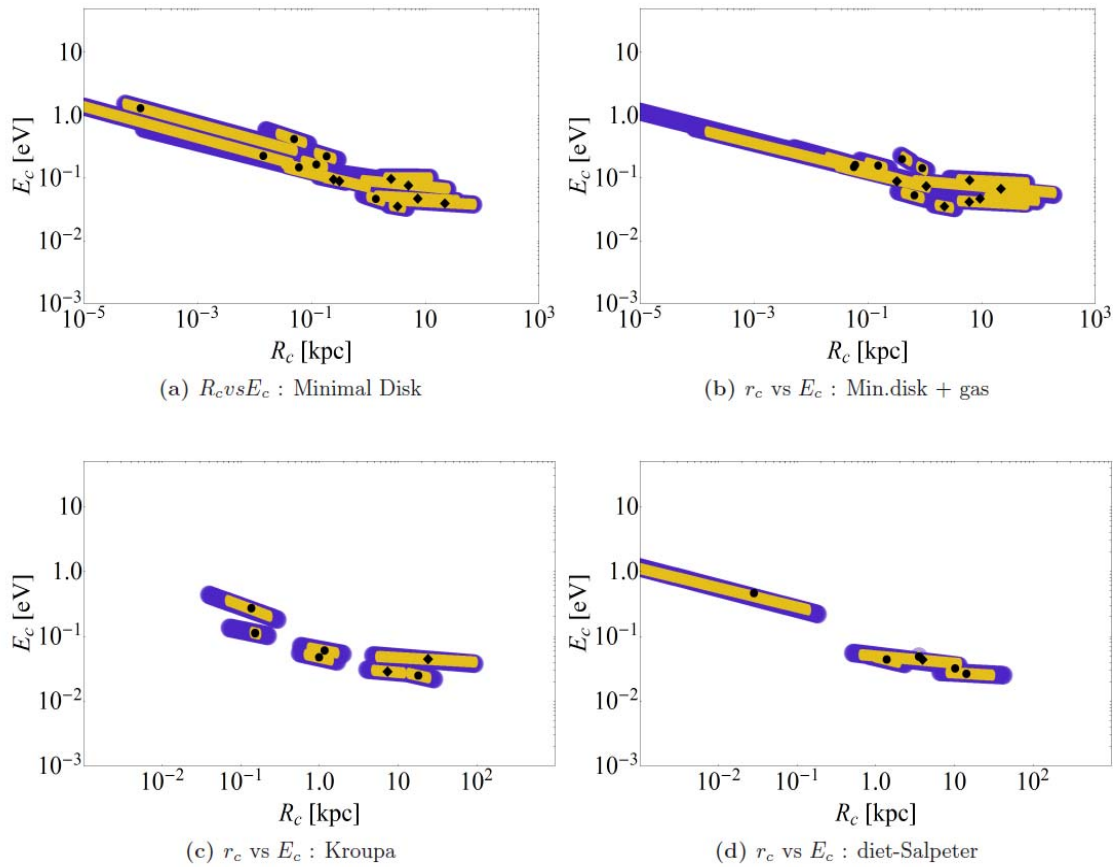


FIG. 3: This table shows the 2D likelihood contours for the BDM parameters ρ_0 and r_c for galaxies with $r_c = r_s$, group B. The different colors in each figure represent the 1 σ and 2 σ confidence levels. Columns from left to right corresponds to minimal disk, minimal disk + gas, and Kroupa. When more mass components

Summary of 2-D contour plots of E_c vs r_c core for diff. Mass models



Minimum Disk

$$E_c = 0.11 \times 10^{\pm 0.46} \text{ eV} = 0.11^{+0.22}_{-0.07} \text{ eV}$$

$$r_c = 300 \times 10^{\pm 1.37} \text{ pc,}$$

FIG. 1: We plot the values of r_c vs E_c for each galaxy and different mass models. Circles represent galaxies

BDM Statistics											
Mass Models (1)	Energy E_c						Core r_c				
	\tilde{E}_{c_n} (2)	E_{c-} (3)	E_c (4)	E_{c+} (5)	$\sigma(E_c)$ (6)	$\log_{10} \rho_c$ (7)	\tilde{r}_{c_n} (8)	r_{c-} (9)	\hat{r}_c (10)	r_{c+} (11)	$\sigma(r_c)$ (12)
Min.Disk	0.21	0.04	0.11	0.33	0.46	8.85	3.02	0.01	0.30	7.02	1.37
Min.Disk+gas	0.10	0.05	0.08	0.15	0.25	8.35	3.81	0.15	0.98	6.60	0.83
Kroupa	0.08	0.03	0.06	0.13	0.33	7.65	6.59	0.16	1.48	13.73	0.97
diet-Salpeter	0.13	0.02	0.07	0.21	0.47	7.92	5.85	0.17	1.70	17.37	1.01

Kroupa

$$E_c = 0.06 \times 10^{\pm 0.33} \text{ eV} = 0.06^{+0.07}_{-0.03} \text{ eV};$$

$$r_c = 1.48 \times 10^{\pm 0.97} \text{ kpc,}$$

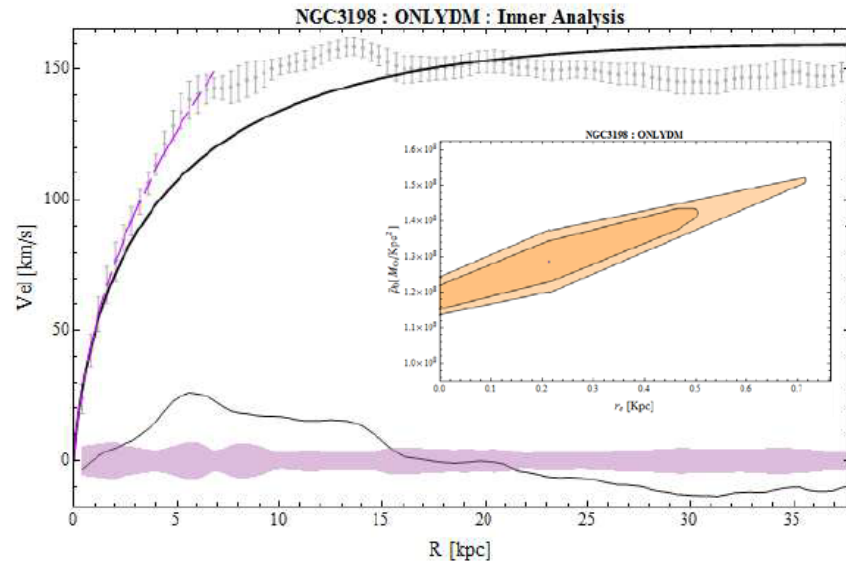
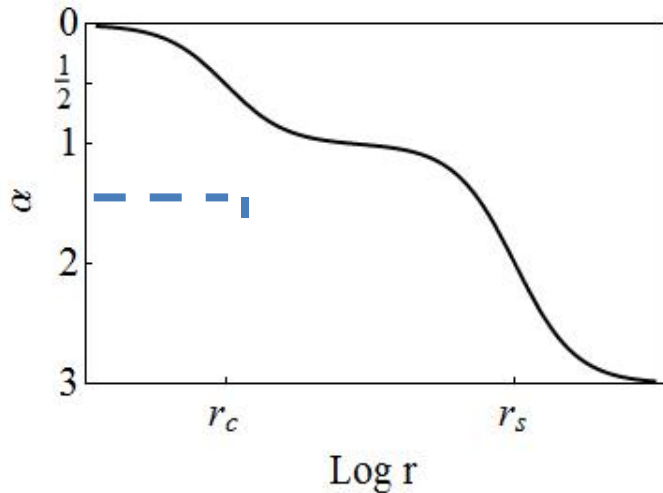
INNER ANALYSIS

useful to extract information on the inner region of galaxies

$$\rho_{\text{int}} = \frac{2\rho_c}{\left(1 + \frac{r}{r_c}\right)}$$

$$r_c \approx 1.3 \text{ kpc}$$

$$E_c^4 = \rho c \approx (0.06 \text{ eV})^4$$



(a) Fit and Difference

$$\alpha \equiv -\frac{d \log \rho}{d \log r} = \frac{r/r_c(1 + 3r/r_s + 2r_c/r_s)}{(1 + r/r_c)(1 + r/r_s)}$$

$$\rho_\alpha = \rho_0 r^{-\alpha}$$

NFW has $\alpha = 1$

$$\alpha \begin{cases} 0 & r = 0 \\ 1/2 & r = r_c \\ 1 & r_c < r < r_s \end{cases} \quad \alpha \leq 0.52$$

INNER ANALYSIS

Inner Analysis - ρ_{in}

Galaxy	Min. Disk.					Min.Disk+gas					Kroupa				
	R_m	r_c	$\log_{10} \rho_c$	χ_{inn}^2	χ_t^2	R_m	r_c	$\log_{10} \rho_c$	χ_{inn}^2	χ_t^2	R_m	r_c	$\log_{10} \rho_c$	χ_{inn}^2	χ_t^2
G.A. NGC 3621	3.32	< 0.01	$9.89^{+10.0}_{-8.19}$	1.24	2.43	3.32	$0.03^{+0.01}_{-0.01}$	$9.46^{+8.87}_{-7.59}$	1.43	1.97	3.32	< 0.02	$9.41^{+7.6}_{-7.22}$	1.54	4.13
IC 2574	11.6	$3.27^{+0.11}_{-0.12}$	$6.72^{+5.29}_{-5.32}$	0.63	0.54	11.6	$2.22^{+0.12}_{-0.12}$	$6.72^{+5.47}_{-5.46}$	0.58	0.39	11.6	$7.37^{+0.29}_{-0.28}$	$6.35^{+5.01}_{-5.01}$	0.79	0.75
NGC 2366	2.28	$7.39^{+0.82}_{-0.70}$	$7.22^{+6.38}_{-6.32}$	0.04	1.41	2.08	$9.42^{+1.12}_{-0.98}$	$7.21^{+6.41}_{-6.37}$	0.07	1.20	0.99	$24.2^{+5.55}_{-4.10}$	$7.12^{+6.60}_{-6.52}$	0.12	1.86
NGC 2903	2.11	$5.07^{+0.88}_{-0.73}$	$8.06^{+7.41}_{-7.32}$	1.61	18.0	1.81	$22.0^{+7.33}_{-4.78}$	$7.84^{+7.47}_{-7.34}$	0.73	21.4	2.72	$81.3^{+5.10}_{-7.20}$	$6.44^{+4.80}_{-4.80}$	14.7	39.3
G.B NGC 2976	2.57	$0.25^{+0.02}_{-0.01}$	$8.44^{+7.31}_{-6.67}$	1.14	0.99	2.57	$1.07^{+0.01}_{-0.18}$	$8.01^{+6.51}_{-7.24}$	2.88	0.83	2.57	$197^{+6.68}_{-6.07}$	$7.40^{+6.07}_{-6.01}$	1.18	423
NGC 3198	3.61	$0.31^{+0.09}_{-0.09}$	$8.34^{+7.78}_{-7.60}$	0.03	1.76	3.21	$0.33^{+0.10}_{-0.10}$	$8.33^{+7.80}_{-7.08}$	0.04	3.16	7.23	$191^{+18.0}_{-15.2}$	$6.63^{+5.73}_{-5.69}$	10.5	15.8
NGC 3521	2.18	$1.95^{+0.12}_{-0.35}$	$8.47^{+7.36}_{-7.80}$	15.2	45.7	1.87	$6.19^{+0.67}_{-0.58}$	$8.40^{+7.63}_{-7.45}$	13.4	69.3	5.60	> 10^3	< 2	48.9	51.6
NGC 925	6.02	$22.3^{+0.73}_{-0.70}$	$6.91^{+5.54}_{-5.54}$	0.21	0.62	6.02	$6.10^{+0.27}_{-0.26}$	$7.01^{+5.75}_{-5.70}$	0.25	0.98	6.02	> 10^3	$6.31^{+5.01}_{-5.01}$	1.98	44.0
G.C NGC 2403	2.04	< 0.01	$10.4^{+10.7}_{-8.77}$	1.86	1.94	2.04	< 0.004	$10.5^{+10.9}_{-8.83}$	1.87	1.89	2.04	> 10^5	$5.27^{+4.3}_{-4.3}$	228	211
NGC 5055	0.73	< 0.003	$11.3^{+12.4}_{-10.3}$	-	4.65	0.73	< 0.003	$11.3^{+12.4}_{-10.3}$	-	3.84	0.73	> 10^5	$6.7^{+5.2}_{-5.2}$	-	10.1

$$\rho_{int} = \frac{2\rho_c}{\left(1 + \frac{r}{r_c}\right)}$$

TABLE V: We show the values obtained from the inner analysis, for all the mass model (except diet-Salpeter, cf. Appendix A), with the profile ρ_{in} . R_m is the maximum radius to consider when making the inner-core analysis. The core radius r_c is given in [kpc] and the logarithm of the central density ρ_c in [M_\odot/kpc^3], both parameters obtained from the inner analysis in which we fit the profile $\rho_{in} = 2\rho_c(1 + r/r_c)^{-1}$ to the data below R_m where we obtained the goodness-of-fit χ_{red}^2 . Using the parameters (r_c , r_s , and ρ_0) obtained from the analysis of the complete set of data and the ρ_{bdm} , we compute χ_t^2 which is the contribution of the data

$$\rho_\alpha = \rho_0 r^{-\alpha}$$

Galaxy	Inner Analysis - ρ_α											
	α	Min.Disk			Min.Disk.+gas				α	Kroupa		
		$\log_{10} \rho_0$	χ_{red}^2	r_c	α	$\log_{10} \rho_0$	χ_{red}^2	r_c		$\log_{10} \rho_0$	χ_{red}^2	r_c
IC 2574	0.47	6.93	1.09	11.84	0.54	6.87	1.03	10.22	0.28	6.6	0.98	20.32
NGC 2366	0.19	7.45	0.04	5.55	0.21	7.47	0.05	4.50	0.11	7.47	0.16	4.22
NGC 2903	0.13	8.26	1.03	8.49	0.15	8.46	4.13	6.23	< 0.01	6.76	12.6	74.79
NGC 2976	0.74	8.02	1.17	1.13	0.72	8.06	2.02	1.18	< 0.01	5.17	381	130.9
NGC 3198	0.76	7.99	0.12	1.90	0.74	8.00	0.13	1.70	0.03	6.92	9.77	126.5
NGC 3521	0.01	8.66	6.77	123.8	0.03	8.46	13.7	35.5	0.90	< 1	45.8	2.60
NGC 925	0.22	7.25	0.15	13.9	0.20	7.22	0.16	15.3	1.60	4.63	36.0	1.32

$$\alpha \begin{cases} 0 & r = 0 \\ \frac{1}{2} & r = r_c \\ 1 & r_c < r < r_s \end{cases}$$

$$\alpha \leq 0.52$$

TABLE VI: Fits with the profile $\rho = \rho_0 r^{-\alpha}$ c.f. Eq. (20) for galaxies belonging to group G.B. for all the mass models (except diet-Salpeter, cf. Appendix A). The distance until which we consider the observations is given by R_m given in Table V. The magnitude of the slope of the rotation curve is given by the dimensionless parameter α . The r_c is the core radius, given in Kpc, obtain based on the value of α and Eq. (21).

Summary and Conclusions

- BDM DARK MATTER behave as :
 - HDM at high energy (above E_c)
 - CDM at low energy (below E_c)
- The phase transition E_c can be determined from gauge theory,
- i.e. when the bound particles acquire a non perturbative mass
- E_c can also be determined from cosmological data
- We find this high-low energy density transition :
 - i) due to the expansion of our universe
 - ii) in the inner region of galaxies
- BDM has a cut in the power spectrum
- BDM has cored DM profile (instead of the cuspy CDM NFW profile)
- Solves the problems of CDM: substructure and cuspy profile
- Has an equivalent or better fit to the cosmological data than CDM

References

References:

- **BDM Dark Matter: CDM with a core profile and a free streaming scale**
A. de la Macorra, [Astropart.Phys. 33:195-200,2010.](#)
- **Galactic Phase Transition at $E_c = O(0.1 \text{ eV})$ from Rotation Curves of Cored LSB and non perturbative Dark Matter Mass.**
A. de la Macorra, J. Mastache, J. Cervantes.
PRD Rapid Communications: [Phys.Rev. D84 \(2011\) 121301](#)
- **Core-Cusp revisited and Dark Matter Phase Transition Constrained at 0.1 eV with LSB Rotation Curve.**
J. Mastache, A. de la Macorra, J. Cervantes [arXiv:1107.5560](#)